NUMERICAL INVESTIGATION OF USING DIFFERENT ARRANGEMENT OF FIN SLIDES ON THE PLATE-FIN HEAT SINK PERFORMANCE

by

Mostafa A. H. ABDELMOHIMEN[a,b*], Khalid ALMUTAIRI[c], Mohamed A. ELKOTB[a,d], Hany E. ABDELRAHMAN[b], and Salem ALGARNI[a]

[a] Mechanical Engineering Department, College of Engineering, King Khalid University, Abha, Saudi Arabia
[b] Mechanical Engineering Department, Shoubra Faculty of Engineering, Benha University, Cairo, Egypt
[c] Mechanical Engineering Department, Engineering College, University of Hafr Al Batin, Hafr Al Batin, Saudi Arabia
[d] Mechanical Engineering Department, College of Engineering, Kafrelsheikh University, Kafrelsheikh, Egypt

Original scientific paper
https://doi.org/10.2298/TSCI201004065A

Cutting fins of the plate heat sinks into multi-numbers of slides instead of one slide fin is a technique to improve the performance of the heat sink. One, two, three, and four slides have been studied numerically. The slides have been arranged in staggered arrangement. The study has been carried out on two different flow directions (impinging and parallel). The performance of the heat sink under the studied conditions has been represented through calculation of heat sink effectiveness, thermal resistance, pressure drop, pumping power, and Nusselt number. The studied range of Reynolds number is from 1333 to 5334. The results show that parallel flow gives lower thermal resistance than impinging flow for all studied cases. The pumping power required for high Reynolds number in case of parallel flow increases by around 155% with Case 4 (four slides) as compared by Case 1 (one slide), while it is slightly affected in case of impinging flow. Using three slides with impinging flow represents an acceptable decrement in thermal resistance with low change in the required pumping power. In case of parallel flow, the resulting change in the heat sink performance, as the number of slides increases, is not proportional to the large increase in the pumping power.

Key words: *heat sinks, fins, thermal resistance, impinging flow, parallel flow*

Introduction

Heat sinks are widely used in electronics equipment, air-conditioning, and many cooling systems as a heat dissipation device. The performance of the heat sink is affected by many parameters. Fin shape and profile are important parameters considered for designing of the fins. Plate and pin fins are assumed to be the best cost and manufacturing techniques available [1]. Kim *et al.* [2] represented an experimental and numerical study on both plate-fin and pin-fin heat sinks subjected to an impinging flow. Many researchers pay attention to improve

* Corresponding author, e-mail: mostafa.abdelmohimen@feng.bu.edu.eg

the performance of the plate-fin heat sinks [3-6]. Huang and Tung [7] studied numerically and experimentally the performance of the deformed wavy-shaped heat sinks. Duan *et al.* [8] represented analysis of flow characteristics and pressure drop for an impinging plate fin heat sink with elliptic bottom profiles. Hosseinirad *et al.* [9] studied the effects of splitter shape on thermal-hydraulic characteristics of plate-pin-fin heat sink. Two new configurations of splitter, namely arched and wavy, are proposed to improve the overall hydrothermal performance of heat sinks. Alfellag *et al.* [10] investigated numerically the effect of an inclined slotted plate-fin mini-channel heat sink with triangular pins on laminar convection heat transfer and fluid-flow using a conjugate heat transfer model. The results showed that the full height slot with an inclination angle of 55° enhanced the Nusselt number and the hydrothermal performance factor up to 1.5 and 1.43, respectively. Abdelmohimen *et al.* [11] investigated numerically the effect of using through rod configurations on the heat transfer of plate-fin heat sink. They concluded that using of four rods through fins is the optimum case along with the studied range of Reynolds number. Wiriyasart and Naphon [12] represented the heat spreading of liquid jet impingement cooling of cold plate heat sink with different fin shapes (rectangular, circular, conical). The results showed that the fin shapes of the heat sink influencing its total thermal resistance but small decrement in heat spreading resistance. Freegah *et al.* [13] studied numerically heat transfer enhancement in plate-fin heat sinks with fillet profile. The investigation develops a new thermal design for plate-fin heat sinks with fillet profile so that the removed material from the base, to generate fillet, is attached to the plate-fins in the form of half-round pins. Subramanian *et al.* [14] investigated experimentally micro-channel heat sink with modified hexagonal fins. Investigation of using PCM to improve the performance of heat sinks attracts attention in the recent time [15-18]. Taghilou and Khavasi [18] represent a numerical investigation on the PCM-filled heat sink with an emphasis on the ambient convective heat transfer. The boundary conditions of heat sink also attract attentions of some researchers [19, 20].

Bar-Shalom [19] provided a guidance to determine the thermal design parameters to improve the performance of high altitude avionics cooling systems and to identify the flight condition causing critical thermal conditions.

Elsayed *et al.* [20] represented the thermal performance of an enhanced air-cooled heat sink system, comprising of a parallel plate-fin heat sink with a guide plate installed to alter the bypass flow, was analyzed for fan-driven convection conditions at various altitudes from sea level to 12000 m. Many researches do not limit to pin-fin and plate-fin heat sinks. Shaeri and Bonner [21] studied the heat transfer and pressure drop in laterally perforated-finned heat sinks across different flow regimes. Li *et al.* [22] represented an investigation of natural-convection heat transfer around a radial heat sink with a perforated ring. Ozsipahia *et al.* [23] numerically investigated the hydraulic and thermal performance of a honeycomb heat sink. Perforated rectangular fins were also studied [24-26]. Nair [27] presented a simple method to improve natural-convection heat transfer performance of horizontal-base straight-fin heat sink by adding partial shroud plates on the heat sink at both ends. Li *et al.* [28] enhanced the performance of heat sink by using aluminum foam through integrated pin fins.

Most of previous studies enhancement of heat sinks depend on increasing the subjected area of the heat sinks or modifying the shape of the fins through using new technologies of manufacturing. The target of the present work is to investigate the enhancement that can be achieved to the traditional plate fin heat sink without make an additional manufacturing cost or more materials construction. The current study depends on separating the traditional fins into multi-numbers of slides of fins and rearranging them in a staggered arrangement. This technique combines between the advantages of plate fin heat sink and pin fin heat sink. The study

is carried out under impinging and parallel flow directions. Four cases with different number of slides are investigated to obtain the optimum number of slides that can be used.

Numerical simulation

Studied models

The current study depends on cutting the fins of the plate-fin heat sink into different slides of fins. Figure 1 shows a heat sink with one slide of fins (Case 1) which is used as the baseline case.

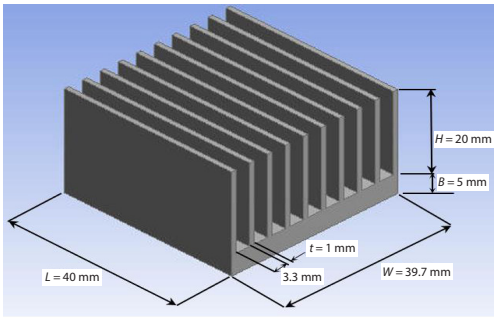

Figure 1. Baseline case (Case 1) with dimensions

The complete fin has been cut into two, three and four slides and rearranged as staggered arrangement to give Cases 2-4, respectively as shown in fig. 2. For staggered arrangement, even the volume of the heat sink is the same, the surface area increases because after cutting the fin slide into more than one slide, the thickness of the fin represents more area according to the number of slides. Two different flow directions, impinging and parallel flows, have been studied. The impinging flow domain has one inlet and two outlets while the parallel flow has one inlet and one outlet. The Reynolds number is calculated according to the flow rate through the inlet area and it will be the same for both flow directions. Figure 3 shows the studied flow directions.

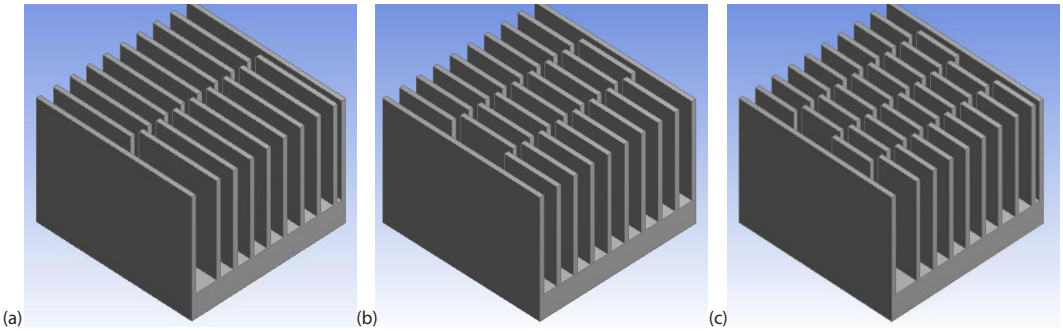

Figure 2. Studied cases with different configurations of different numbers of slides; (a) Case 2 (two slides), (b) Case 3 (three slides), and (c) Case 4 (four slides)

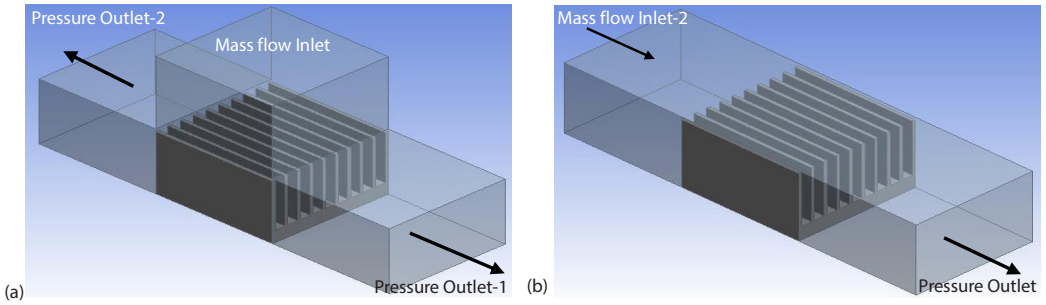

Figure 3. Studied directions of the air-flow with boundary conditions; (a) impinging flow direction and (b) parallel flow direction

Mesh generation

The fluid domain has been created to investigate the required study as shown in fig. 3. Geometry of construction, mesh, discretization, and solving of governing equations has been carried out by using ANSYS FLUENT 17.2. Table 1 represents the grid independency results for the base temperature and thermal resistance with different mesh values. The size of mesh is ranged from 116479 elements to 2657672 elements for baseline case. The mesh value of 752039 is selected to carry out the current study.

Table 1. Results of the grid independency study

Mesh	Number of elements	Base temperature [°C]	R_{th}	Difference in temperature with previous [%]	Difference in R_{th} with previous [%]
Mesh 1	116479	65.715	1.457	–	–
Mesh 2	221571	65.361	1.300	0.10	10.77
Mesh 3	752039	65.031	1.271	0.10	2.19
Mesh 4	2657672	65.402	1.271	–0.01	0.03

Boundary conditions and modelling

The boundary conditions are considered like the experimental work of Kim *et al.* [2]. The air-flow at inlet has four values of Reynolds number (1333, 2667, 4000, and 5334) at 25 °C. The corresponding mass-flow rate is calculated based on the inlet condition and the inlet hydraulic diameter with turbulence intensity of 5%. The value of mass-flow rate for impinging flow direction is different from that of parallel flow direction due to difference in inlet area, tab. 2. Reynolds number may be calculated by using eq. (1). The air properties, according to Kim *et al.* [2], are taken as density $\rho_a = 1.1774$ kg/m^3, dynamic viscosity $\mu_a = 1.8462 \cdot 10^{-5}$ kg/ms, specific heat $c_{p,a} = 1.0057 \cdot 10^3$ J/kgK, and thermal conductivity $k_a = 0.02624$ W/mK. The heat sink is made of aluminum alloy 6061 with thermal conductivity $k_s = 171$ W/mK. The base of the heat sink is subjected to constant heat flux of 18750 W/m^2. The outside walls of the heat sink as well as the duct walls are assumed adiabatic walls:

$$\mathrm{Re}_{D_h} = \frac{\rho U_{\mathrm{avr}} D_{\mathrm{h}}}{\mu} \tag{1}$$

Table 2. Studied range of mass-flow rate and corresponding Reynolds number

No.	Corresponding Reynolds number	Mass-flow rate [kgs^{-1}]	Mass-flow rate [kgs^{-1}]
		Impinging flow direction	Parallel flow direction
1	1333.63	0.000981	0.0007965
2	2667.26	0.001962	0.001593
3	4000.89	0.002944	0.0023895
4	5334.52	0.003925	0.003186

The shear-stress transport (SST) k-ω model has been selected to carry out the numerical analysis. More details about reasons for selecting this model and the governing equations of it has been represented in [11].

Calculation procedure

To validate the present work and estimate the improvement of heat sink performance, thermal resistance has been used and calculated by:

$$R_{th} = \frac{1}{\bar{h} A_T} \tag{2}$$

where A_T is the total area of the heat sink subjected to the fluid-flow and $\bar{h}$ – the mean heat transfer coefficient.

Calculation of the mean heat transfer coefficient is done by using eq. (3). The total area for the Case 1 which has one slide by using eq. (4). For Cases 2-4, eq. (5) is used to calculate the total area, a new term is included in the equation of total area to show the effect of fin thickness due to separation of fins:

$$\bar{h} = \frac{Q}{A_T \left(T_\mathrm{b} - T_\mathrm{avr} \right)} \tag{3}$$

$$A_{T_{\text{one slide}}} = WL + 2H \left[L\left(N_f - 1 \right) + tN_f \right] + 2BW \tag{4}$$

$$A_T = WL + 2H \left[L\left(N_f - 1 \right) + tN_f \right] + 2BW + N_s tH \left(N_f - 2 \right) \tag{5}$$

where Q is the heat transfer rate calculated by eq. (6), T_b – the fin base temperature, and T_avr – the average air temperature given by eq. (7). The W and L are the width and length of the heat sink, respectively, N_f, H, and t are the fins number, height above the base, and thickness, respectively. While B is the base height. The N_s is the number of slides starting from 2:

$$Q = \dot{m}_\mathrm{a} c_{p,\mathrm{a}} \left(T_\mathrm{out} - T_\mathrm{in} \right) \tag{6}$$

$$T_\mathrm{avr} = \frac{\left(T_\mathrm{out} - T_\mathrm{in} \right)}{2} \tag{7}$$

where $\dot{m}$ and $c_{p,\mathrm{a}}$ [kgs^{-1}] are the mass-flow rate and specific heat of air at the average temperature T_avr, respectively, T_out and T_in – the outlet and inlet temperature of air, respectively.

Nusselt number is used to represent the performance of the heat sink. It can be calculated by using eq. (8):

$$\overline{\mathrm{Nu}} = \frac{\bar{h} D_\mathrm{h}}{k_\mathrm{a}} \tag{8}$$

where D_h is the hydraulic diameter of the inlet and K_a – the thermal conductivity of the air based on the average temperature of air. The required power for pumping the flow depends on calculating of the pressure drop, Δp – the pressure drop and the pumping power can be calculated by using eqs. (9) and (10):

$$\Delta p = P_\mathrm{out} - P_\mathrm{in} \tag{9}$$

$$P_P = \frac{\Delta p \dot{m}_\mathrm{a}}{\rho_\mathrm{a}} \tag{10}$$

Results and discussion

Validation of the model

The current results of Case 1, which have been taken as the baseline case, are compared with the experimental work of Kim *et al.* [2] to validate the numerical model. Impingement flow at different mass-flow rate with baseline case is used to carry out the required comparison. A good agreement between the numerical and experimental results for thermal resistance with maximum discrepancy of about 2.8% has been shown in fig. 4. a good agreement has also been obtained with the pressure drop with about 10% discrepancy as shown in fig. 5. An acceptable explanation for the difference may be due to thermal losses and measurement errors [4]. As a result of the validation, the numerical model can be assumed suitable for carrying out the current study.

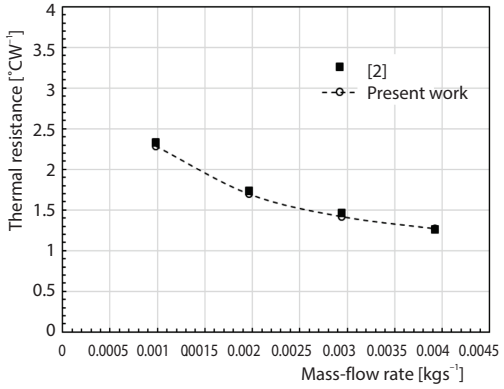

Figure 4. Validation of present work for thermal resistance with baseline case, impingement flow direction

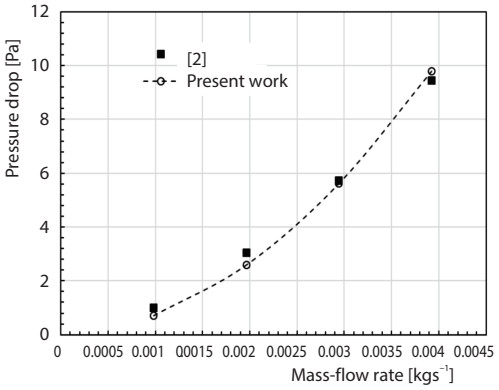

Figure 5. Validation of present work for pressure drop with baseline case, impingement flow direction

Effectiveness of the heat sink

The temperature reduction of the heat sink surface can be explained by using effectiveness term [11]. Effectiveness can be calculated by using eq. (11). The cooling is not effective if the value of the effectiveness closes to zero. The more the effectiveness the more cooling has been achieved.

$$\varepsilon = \frac{T_{\mathrm{b}} - T_{\mathrm{s}}}{T_{\mathrm{b}} - T_{\mathrm{in}}} \tag{11}$$

Figures 6 shows the detailed effectiveness of the heat sink at lowest and highest studied Reynolds number of 1334 and 5334 for the studied cases with impinging and parallel flow directions. For impinging flow direction, fig. 6(a). Shows that, at high Reynolds number, the number of slides represents a significant effect on the effectiveness. While at low Reynolds number, there is lower effect as the number of slides increases. It is noted also, the effect of flow appears on the right and left side of the heat sink because the flow is coming normal to the heat sink fins and moving to outlet on the right and left directions. For parallel flow direction, fig. 6(b) shows the same effect of Reynolds number. *i.e.* the higher Reynolds number, the higher effectiveness and the higher number of slides, the higher effectiveness. But the higher effectiveness appears near the inlet of the air-flow rather than the outlet of it because at the inlet the

parallel fluid-flow has the lowest temperature causing higher heat transfer. While as the air is moving through the heat sink fins the air temperature increases gradually causing lower heat transfer from the heat sink at outlet. To explain the effect of using different number of slides and the flow directions, thermal resistance, pressure drop, and Nusselt number should be represented and compared.

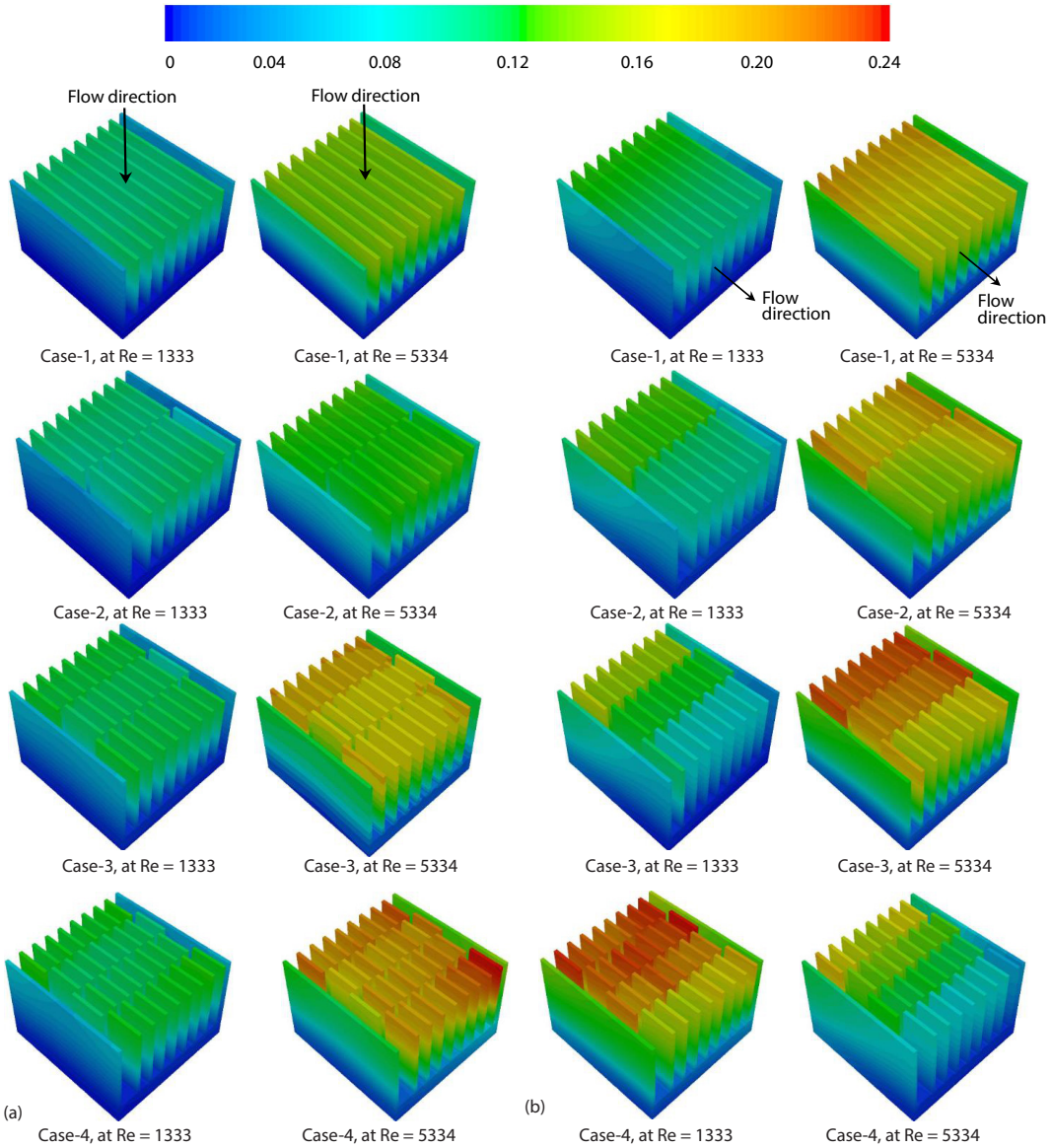

Figure 6. The detailed heat sink effectiveness for studied cases with impinging and parallel flow direction; (a) impinging flow direction and (b) parallel flow direction

Thermal resistance pressure drop, and Nusselt number

The thermal resistance of the heat sink for the studied cases has been represented in fig. 7. The parallel flow shows lower thermal resistance as compared to impinging flow for all studied cases. The reduction of the thermal resistance for parallel flow is about 50% at Re = 1333 and 44% at Re = 5334 as compared with impinging flow direction. It is clear also as the Reynolds number increases, the thermal resistance decreases for all studied cases. The figure shows the number of slides slightly affects the thermal resistance with high Reynolds number in parallel flow, whereas the slides have significant effect in impinging flow. For impinging flow, Cases 2 and 4 show higher thermal resistance as compared with Case 1 (baseline case). Case 2 thermal resistance increases by 7% of Case 1 thermal resistance at Re = 1333 and about 12.4% at Re = 5334 and Case 4 thermal resistance decreases by 4.6% at Re = 1333 and increases for other values of Reynolds numbers by about 4.2% at Re = 5334. While Case 3 shows lower thermal resistance for all studied values of Reynolds number starting from 4.2% reduction at Re = 1333 to 6% reduction at Re = 5334. It is clear from that, the lowest thermal resistance with impinging flow is given by Case 3 although Case 4 gives the lowest effectiveness as represented in fig. 6(a). This result can be explained as the thermal resistance depends on the base temperature not on the fins temperature and with Case 4 the air gains more heat as it moves between fins and before reaches the fin base due to higher turbulence as compared with Case 3. This effect is more clearly as Reynolds number increases while the turbulence between fins is low with low Reynolds number. So, the thermal resistance shows approximately the same value for Cases 3 and 4. For parallel flow the lowest thermal resistance is given by Case 4. At Re = 1333, the thermal resistance is reduced by 4.5%, 6%, and 12.15% for Cases 2-4, respectively. While at Re = 5334, it increases by 4.9% for Case 2 and reduces by 4.5% and 2.17% for Cases 3 and 4, respectively. The reduction in thermal resistance in case of parallel flow is not significant as the number of slides increase because as the number of slides affects slightly on the contact between the air-flow and the heat sink base. While it affects significantly on the contact between the air-flow and the fins surfaces as it moves parallel to them as shown in fig. 6(b). The pressure drop through the heat sink is an important parameter to analyze the feasibility of using slides. Figure 8 shows the pressure drop through the heat sink for all studied cases. For impinging flow, the pressure drop value is not affected by increasing the number of slides for all studied values of Reynolds number. This is because the flow is normal to the

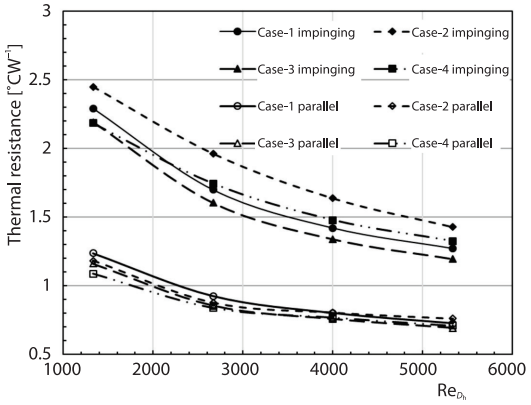

Figure 7. The thermal resistance of the heat sink for impinging and parallel flow directions

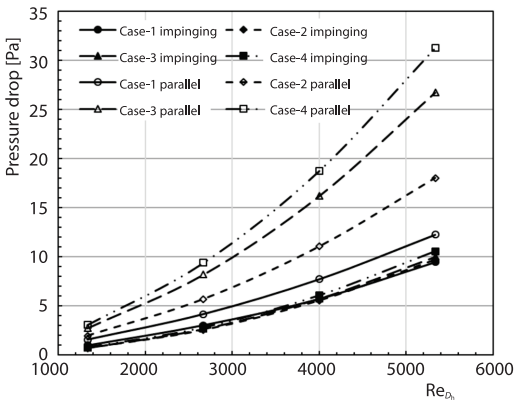

Figure 8. The pressure drop through the heat sink for impinging and parallel flow directions

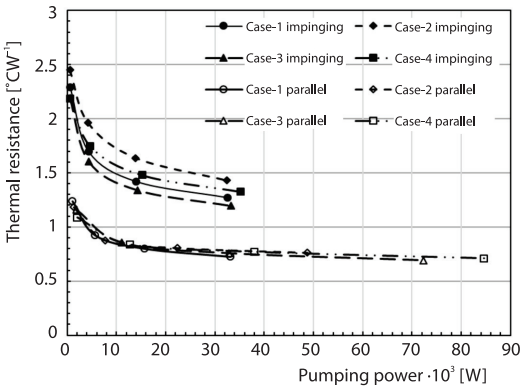

Figure 9. The thermal resistance *vs.* pumping power of the heat sink for impinging and parallel flow directions

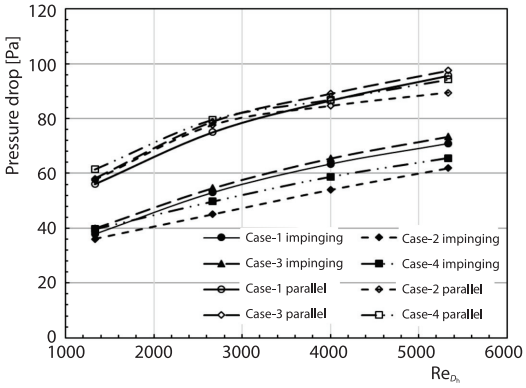

Figure 10. Nusselt number of the heat sink for impinging and parallel flow directions

base of the heat sink and because the flow meets all the fin slides at the same plane and the same time. While for parallel flow, the pressure drop is highly affected by the number of slides, especially with high Reynolds number. With parallel flow, the air-flow pressure drops as it meets the first row of slides, then more pressure drop is achieved as the number of slides rows increases (scattering effect). The percentage of increasing of the pressure drop with impinging flow reaches 8% for Re = 5334 as compared with Case 1 (baseline case). While with parallel flow, the percentage of increasing of pressure drop starts from 25% at Re = 1333 for Case 2 to reach to 155% at Re = 5334 for Case 4.

To determine the optimum case of using different number of slides in view of pumping power and heat transfer, it is important to represent the effect of using fin slides on the pumping power and Nusselt number. Figure 9 shows the thermal resistance *vs.* the pumping power for all studied cases. The parallel flow pumping power increases with significant values as the number of slides increases while there is no significant change in the thermal resistance. For impinging flow, the reduction of thermal resistance due to use slides does not meet a significant change in pumping power. Figure 10 represents the effect of using slides on the Nusselt number. The impinging flow shows lower Nusselt number than that of parallel flow for all studied cases. As Reynolds number increases, Nusselt number increases. The highest Nusselt number for impinging flow is given by Case 3. While for parallel flow, the highest Nusselt number is given by Case 4 at low Reynolds number and by Case 2 at high Reynolds number but without much change in values.

Conclusion

The effect of cutting fins of plate heat sink into multi-numbers of slides has been investigated in this research. Four cases have been studied numerically including one, two, three, and four slides, respectively. The study carried out for impinging and parallel flow directions. The results show that parallel flow gives lower thermal resistance than impinging flow for all studied cases. The pressure drop through heat sink increases significantly as the number of slides increases for parallel flow, but it is slightly affected with impinging flow. The pumping power required for high Reynolds number in case of parallel flow increases by around 155% with Case 4 (four slides) as compared to Case 1 (one slide). While it is slightly affected in case of impinging flow. An acceptable reduction in thermal resistance is achieved with impinging flow Case 3 (three slides) with no much change in the required pumping power. Using slides

with parallel flow does not give the required enhancement of the thermal resistance related to the much change of the pumping power.

Acknowledgment

The authors extend their appreciation the Deanship of Scientific Research at King Khalid University for funding this work through Research Group Project under grant number (R.G.P1./95/40).

Nomenclature

A_c – cross-section area at inlet
A_T – total surface area of the heat sink
B – base height [m]
D_h – hydraulic diameter [m] (= $4A_c/P$)
H – height of the heat sink, above the base [m]
$\bar{h}$ – mean heat transfer coefficient
L – length of the heat sink, [m]
k – thermal conductivity, [$Wm^{-1}K^{-1}$]
$\dot{m}$ – mass-flow rate, [kgs^{-1}]
N_f – number of fins
Nu – Nusselt number
P – perimeter of inlet section
P_P – pumping power, [W]
Re – Reynolds number
R_{th} – thermal resistance
Δp – pressure drop, [Pa]
T – temperature, [K]
t – fin thickness, [m]
U – velocity at inlet
W – width of the heat sink, [m]

Greek symbols

ρ – air density, [kgm^{-3}]
μ – dynamic viscosity of the air, [Pas]

Subscripts

a – air
avr – average
b – base
h – hydraulic
in – air inlet
out – air outlet
s – heat sink surface

Superscripts

$\bar{}$ – averaged

References

[1] Khattak, Z., Ali, H. M., Air Cooled Heat Sink Geometries Subjected to Forced Flow: A Critical Review, *International Journal of Heat and Mass Transfer*, *130* (2019), Mar., pp. 141-161
[2] Kim, D. K., *et al*., Comparison of Thermal Performances of Plate-Fin and Pin-Fin Heat Sinks Subject to an Impinging Flow, *Int. Journal of Heat and Mass Transfer*, *52* (2009), 15-16, pp. 3510-3517
[3] Wong, K. C., Indran, S., Impingement Heat Transfer of a Plate Fin Heat Sink with Fillet Profile, *International Journal of Heat and Mass Transfer*, *65* (2013), Oct., pp. 1-9
[4] Hussain A. A., *et al*., Numerical Investigation of Heat Transfer Enhancement in Plate-Fin Heat Sinks: Effect of flow direction and fillet profile, *Case Studies in Thermal Engineering*, *13* (2019), Mar., 100388
[5] Jeon, D., Byon, C., Thermal Performance of Plate Fin Heat Sinks with Dual-Height Fins Subject to Natural-Convection, *International Journal of Heat and Mass Transfer*, *113* (2017), Oct., pp. 1086-1092
[6] Saravanakumara T., Kumar, D. S., Performance Analysis on Heat Transfer Characteristics of Heat SINK with Baffles Attachment, *International Journal of Thermal Sciences*, *142* (2019), Aug., pp. 14-19
[7] Huang, C. H., Tung, P. W., Numerical and Experimental Studies on an Optimum Fin Design Problem to Determine the Deformed Wavy-Shaped Heat Sinks, *Int. Journal of Thermal Sciences*, *151* (2020), 5, 106282
[8] Duan, Z., *et al*., Analysis of Flow Characteristics and Pressure Drop for an Impinging Plate Fin Heat Sink with Elliptic Bottom Profiles, *Applied Science*, *10* (2020), 1, 225,
[9] Hosseinirad, E., *et al*., Effects of Splitter Shape on Thermal-Hydraulic Characteristics of Plate-Pin-Fin Heat Sink (PPFHS), *International Journal of Heat and Mass Transfer*, *143* (2019), Nov., 118586
[10] Alfellag, M. A., *et al*., Numerical Simulation of Hydrothermal Performance of Minichannel Heat Sink Using Inclined Slotted Plate-Fins and Triangular Pins, *Applied Thermal Engineerin*g, *164* (2020), Jan., 114509
[11] Abdelmohimen, M. A., *et al*., Improving Heat Transfer of Plate-Fin Heat Sinks Using through Rod Configurations, *ASME. J. Thermal Sci. Eng. Appl*., *13* (2020), 1, 011003

[12] Wiriyasart, S., Naphon, P., Heat Spreading of Liquid Jet Impingement Cooling of Cold Plate Heat Sink with Different Fin Shapes, *Case Studies in Thermal Engineering*, *20* (2020), Aug., 100638
[13] Freegah, B., *et al*., The CFD Analysis of Heat Transfer Enhancement in Plate-Fin Heat Sinks with Fillet Profile: Investigation of New Designs, *Thermal Science and Engineering Progress*, *17* (2020), June, 100458
[14] Subramanian, S., *et al*., Experimental Investigation of Micro-Channel Heat Sink with Modified Hexagonal Fins, *Journal of Applied Fluid Mechanics*, *12* (2019), 3, pp. 647-655
[15] Sivapragasam, A., *et al*., Experimental Investigation on Thermal Performance of Plate Fin Heat Sinks with NanoPCM, *Thermal Science*, *24* (2020), 1B, pp. 437-446
[16] Arshad, A., *et al*., Experimental Investigation of PCM Based Round Pin-Fin Heat Sinks for Thermal Management of Electronics: Effect of Pin-Fin Diameter, *Int. J. Heat Mass Transfer*, *117* (2018), Feb., pp. 861-872
[17] Pakrouh, R., *et al*., A Numerical Method for PCM-Based Pin Fin Heat Sinks Optimization, *Energy Convers. Manage*., *103* (2015), Oct., pp. 542-552
[18] Taghilou, M., Khavasi, E., Thermal Behavior of a PCM Filled Heat Sink: The Contrast between Ambient Heat Convection and Heat Thermal Storage, *Applied Thermal Engineering*, *174* (2020), June, 115273
[19] Bar-Shalom D., Altitude Effects on Heat Transfer Processes in Aircraft Electronic Equipment Cooling, M. Sc. thesis, Massachusetts Institute of Technology, Cambridge, Mass., USA, 1988
[20] Elsayed, M. L., *et al*., Performance of a Guided Plate Heat Sink at High Altitude, *International Journal of Heat and Mass Transfer*, *147* (2020), 1, 118926
[21] Shaeri, M. R., Bonner, R., Heat Transfer and Pressure Drop in Laterally Perforated-Finned Heat Sinks Across Different Flow Regimes, *Int. Communications in Heat and Mass Transfer*, *87* (2017), Oct., pp. 220-227
[22] Li, B., Jeon, S., Byon, C., Investigation of Natural-Convection Heat Transfer around a Radial Heat Sink with a Perforated Ring, *International Journal of Heat and Mass Transfer*, *97* (2016), C, pp. 705-711
[23] Ozsipahia, M., *et al*., Numerical Investigation of Hydraulic and Thermal Performance of a Honeycomb Heat Sink, *Int. Journal of Thermal Sciences*, *134* (2018), Dec., pp. 500-506
[24] Awasarmol, U. V., Pise, A. T., An Experimental Investigation of Natural-Convection Heat Transfer Enhancement from Perforated Rectangular Fins Array at Different Inclinations, *Experimental Thermal and Fluid Science*, *68* (2015), Nov., pp. 145-154
[25] Aiessa, A. H., *et al*., Enhancement of Natural-Convection Heat Transfer from a Fin by Rectangular Perforations with Aspect ratio of Two, *Int. J. Phys. Sci*., *4* (2009), 10, pp. 540-547
[26] Huang, G. ., *et al*., Enhancement of Natural-Convection Heat Transfer from Horizontal Rectangular Fin Arrays with Perforations in Fin Base, *Int. J. Therm. Sci*., *84* (2014), Oct., pp. 164-174
[27] Nair, D. V., Enhancement of Free Convection from Horizontal-Base Straight-Fin Heat Sink by Partial Shrouding, *ASME. J. Thermal Sci. Eng. Appl*., *12* (2020), 3, 031023
[28] Li, Y., *et al*., Enhancing the Performance of Aluminum Foam Heat Sinks through Integrated Pin Fins, *International Journal of Heat and Mass Transfer*, *151* (2020), Apr., 119376

Paper submitted: October 4, 2020
Paper revised: December 25, 2020
Paper accepted: January 5, 2021